ISSN 2303-4521
Periodicals of Engineering and Natural Sciences *Original Research*
Vol. 11, No. 2, March 2023, pp.102-116

A novel approach for coordinated design of TCSC controller and PSS for improving dynamic stability in power systems

Hayder Okab Alwan
Department of Software, College of Computer Sciences and Information Technology. Wasit University, Iraq

ABSTRACT

The purpose of this article is to present a novel strategy for the coordinated design of the Thyristor Controlled Series Compensator (TCSC) controller and the Power System Stabilizer (PSS). A time domain objective function that is based on an optimization problem has been defined. This objective function takes into account not only the influence that disturbances have on the mechanical power, but also, and this is more accurately the case, the impact that disturbances have on the reference voltage. When the objective function is minimized, potential disturbances are quickly mitigated, and the deviation of the speed of the generator's rotor is limited; as a result, the system's stability is ultimately improved. Particle Swarm Optimization (PSO) and the Shuffled Frog Leaping Algorithm are both components of a composite strategy that is utilized in the process of determining the optimal controller parameters. (SFLA). An independent controller design as well as a collaborative controller design utilizing PSS and TCSC are developed, which enables a direct evaluation of the functions performed by each. The presentation of the eigenvalue analysis and the findings of the nonlinear simulation can help to provide a better understanding of the efficacy of the outcomes. The findings indicate that the coordinated design is able to successfully damp low-frequency oscillations that are caused by a variety of disturbances, such as changes in the mechanical power input and the setting of the reference voltage, and significantly enhance system stability in power systems that are connected weekly.

Keywords: Shuffled Frog Leaping Algorithm, power system stability, PSS, Phillips-Heffron model, TCSC

Corresponding Author:

Hayder Okab Alwan
Software Department, College of Computer Sciences and Information Technology, Wasit University.
Wasit, Iraq
E-mail: h.alwan@uowasit.edu.iq.edu

1. Introduction

It is possible for active power oscillations to take place in power transmission corridors between generating areas because there is insufficient damping of the interconnections with relatively poor tie lines. This is particularly likely to occur during heavy power transfer in large power systems. These oscillations can be triggered by a number of different occurrences, including line failures, line switching, and sudden shifts in the output of the generator. Because of the presence of active power oscillations, there is a constraint placed on the capability of interconnections that can take place between different areas or transmission regions. These oscillations have the potential to increase if there is no damping applied, which could result in the system becoming disconnected [1]. Fixes are frequently attainable through the building of new lines or the enhancement of existing ones; however, these projects are time-consuming and costly to complete. Another option is to install Power System Stabilizers (PSS) on turbines; however, this is not always successful, particularly for low-frequency inter-area power oscillations. This is one of the disadvantages of using PSS. Because of this, the PSS absolutely needs to be accompanied by an efficient instrument. The Thyristor Controlled Series Compensator, or TCSC for short, is an excellent choice in either scenario. Because it does not interact with any of the local oscillation modes, it can be positioned anywhere in the system without affecting its performance as a power oscillation damper, making it a very efficient and cost-effective solution. It's possible that in a few different scenarios, this will turn out to be the best viable choice. Power systems gain a great deal from TCSC's dynamic power flow management, which results in decreased system losses, eliminated line overloads, optimized load

sharing among parallel circuits, reduced risks of sub-synchronous resonance (SSR), dampened active power oscillations, and improved post-contingency stability. All of these benefits are derived from the fact that TCSC is able to eliminate line overloads. Because of this, it has seen widespread use in the construction of lengthy transmission lines [2-6].

Interactions in a network that already has a PSS implemented can become unstable if the PSS and TCSC are not coordinated in their operations. This can cause the interactions to become unstable. As a consequence of this, the PSS and TCSC Power Oscillation Damping (POD) controllers ought to collaborate in order to boost the overall effectiveness of the system [7-10]. POD controllers generally make use of a standard lead-lag controller structure with a washout filter. This is because POD controllers lack the sophistication necessary for fine-tuning, and there is no guarantee that they will remain stable. Today, the Heffron-Phillips model of a synchronous machine is utilized in a variety of research projects for the purpose of analyzing low frequency oscillations and the development of power system stabilizers. In order to conduct an accurate investigation of the suggested methodology, we have included two different cases of study. In the first scenario, the linear model developed by Heffron and Phillips is utilized for a single machine power system. This choice was made due to the linear model's straightforward application and dependable output. The second case is a nonlinear model of a two-area, four-machine power system aggregated with a TCSC and a PSS. This case is intended to demonstrate how the suggested methodology can be applied to a realistic power system. The tuning of PSS and TCSC parameters is a difficult challenge that involves multiple modes and combinatorics. Conventional optimization strategies such as eigenvalue assignment, Genetic Algorithm (GA) and Clonal Selection Algorithm (CSA), and the pole placement procedure have all seen widespread use in the quest to solve the problem described above [11-16]. Only disruptions in mechanical power constitute the primary topic of investigation in this series of studies. In spite of this, a flaw in these studies is that they fail to take into account any of the other potential fluctuations in the objective function. This research investigates the effects, both independently and in conjunction with one another, of implementing PSS and TCSC on the power system. To evaluate the stability of the system following the introduction of two distinct perturbations, a brand-new objective function has been formulated. That is to say, first, a disturbance in mechanical power is applied to the system, and then, secondly, a disturbance in reference voltage is applied to the system. The reaction of the system is then evaluated for the inputted parameters of PSS and TCSC after each of these disturbances has been applied. When the tuning of the parameters is complete, the system will be able to react appropriately to either of the interruptions. This article presents a novel optimization algorithm as a potential solution to the problem that has been outlined. PSO-SFLA is the name given to the novel meta-heuristic population-based optimization method that was developed by combining the Shuffled Frog Leaping Algorithm (SFLA) and the PSO algorithms. This integration resulted in the creation of the proposed method. The PSO-SFLA algorithm's job is to improve the overall system configuration by first optimizing the objective function, then tuning the parameters of the controllers, and ultimately improving the overall system configuration. The following constitutes the general structure of this paper: The single-machine of infinite-bus for the system, also known as SMIB, along with the TCSC and PSS components are discussed in Section 2. In Section 3, a basic introduction to the PSO-SFLA technique is presented, and in Section 4, the issue at hand is described in detail. Section 5 presents the findings obtained from running the simulations. A summary and concluding analysis can be found in the sixth segment.

2. Method

2.1. Power System modeling for TCSC and PSS

A power system for the SMIB is analyzed here; see Fig. 1. A PSS-equipped generator and a TCSC are combined in a series configuration alongside the transmission line to form the system. The transformer reactance is depicted by Xt in the figure,, X_{L1} and X_{L2} both are the transmission lines reactance, V_t as well as V_b stand for a generator terminal and infinite bus voltage correspondingly.

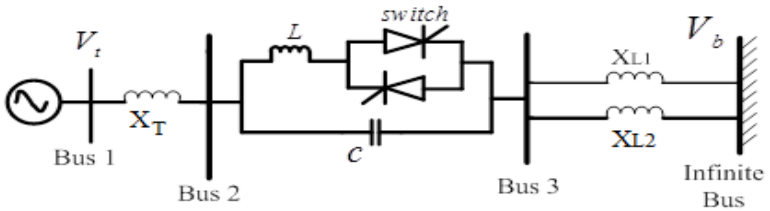

Figure 1. A SMIB power system equipped with TCSC

2.2. Nonlinear equations

The dynamic model of a SMIB with TCSC is defined by four nonlinear differential equations as follows [1, 17]:

$$\dot{\delta} = \omega_0(\Delta\omega) \qquad (1)$$

$$\dot{\omega} = \frac{1}{M}[P_m - P_e - D\Delta\omega] \qquad (2)$$

$$\dot{E}_q^{'} = \frac{1}{T_{d0}^{'}}[-E_q + E_{fd}] \qquad (3)$$

$$\dot{E}_{fd} = \frac{K_A}{1+sT_A}[V_R - V_T + V_s] \qquad (4)$$

$$\dot{\omega} = \frac{1}{M}\ [P_m - P_e - D\Delta\omega]$$

Where,

$$P_e = \frac{E_q^{'}V_b}{X_d^{'}}\sin(\delta) - \frac{V_b^2(x_q - x_d^{'})}{2x_d x_q}\sin(2\delta) \qquad (5)$$

$$E_q = \frac{E_q^{'}X_d}{X_d^{'}} - \frac{V_b(x_q - x_d^{'})}{X_d^{'}}\cos(\delta) \qquad (6)$$

$$V_{td} = \frac{x_q V_b}{X_q}\sin(\delta) \qquad (7)$$

$$V_{tq} = \frac{x_e E_q^{'}}{X_d^{'}} + \frac{x_d^{'}V_b}{X_d^{'}}\cos(\delta) \qquad (8)$$

$$V_t = \sqrt{V_{td}^2 + V_{tq}^2} \qquad (9)$$

With:

$$X_e = X_T + (X_{L1} \| X_{L2}) - X_{TCSC}(\alpha) \qquad (10)$$

$$X_d = x_d + x_e; X_q = x_q + x_e; X_d^{'} = x_d^{'} + x_e \qquad (11)$$

The generator's exciting system is modeled after the IEEE Type-ST1A standard, with a typical lead-lag PSS for added realism. The Type-ST1A excitation mechanism as well as PSS are depicted in Figure 2. For operation, the stimulation system takes in a terminal voltage V_T, a reference voltage V_R, and the PSS signal output VS. We can think of the excitation system's gain and time constant, respectively, as K_A and T_A. Three distinct blocks make up the PSS under consideration here: a gain stage, a signal washout stage, as well as a two-stage phase correction stage. For this analysis, we assume that the dissipation time constant TWP is 10 seconds. The PSS receives the speed variation as an input. Additionally, two parallel phase correction blocks are taken into account to ensure that $T_{2P} = T_{4P} = 0.1$ sec. The remaining parameters to be found are the gain for the stabilizer K_{PS} and constants of time T_{1P} and T_{3P}. The Nomenclature at the conclusion of the paper can be consulted for the explanation of any additional terms.

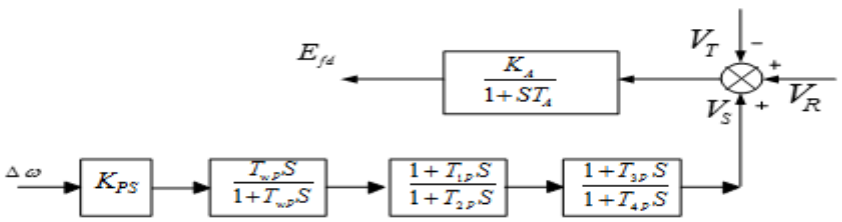

Figure 2. An IEEE-standard ST1A-style excitation device equipped with a PSS

2.3. Linearized model

In order to perform an analysis of the system's behavior during the construction of an electromechanical mode damping stabilizer, it is customarily necessary to use a linearized incremental model centered on a point of equilibrium [1, 18]. We can get the Phillips–Heffron model of the power system with FACTS devices by linearizing Equations (1)–(4) about a working point of the power system. This will allow us to do the following:

$$\Delta\dot{\delta} = \omega_0\Delta\omega \qquad (12)$$

$$\Delta\dot{\omega} = \frac{1}{M}(-K_1\Delta\delta - K_2\Delta E_q^{'} - K_p\Delta\sigma - D\Delta\omega) \quad (13)$$

$$\Delta\dot{E}_q^{'} = \frac{1}{T_{d0}}(-K_3\Delta E_q^{'} - K_4\Delta\delta - K_Q\Delta\sigma + \Delta E_{fd}) \quad (14)$$

$$\Delta\dot{E}_{fd} = \frac{1}{T_A}[-\Delta E_{fd} - K_A(K_S\Delta\delta + K_6\Delta E_q^{'} + K_Q\Delta\sigma)] \quad (15)$$

Where,

$$K_1 = \frac{\partial P_e}{\partial\delta}, K_2 = \frac{\partial P_e}{\partial E_q^{'}}, K_p = \frac{\partial P_e}{\partial\sigma} \quad (16)$$

$$K_3 = \frac{\partial E_q}{\partial\delta}, K_4 = \frac{\partial E_q}{\partial E_q^{'}}, K_Q = \frac{\partial E_q}{\partial\sigma} \quad (17)$$

$$K_5 = \frac{\partial V_t}{\partial\delta}, K_6 = \frac{\partial V_t}{\partial E_q^{'}}, K_V = \frac{\partial V_t}{\partial\sigma} \quad (18)$$

The Phillips-Heffron model of the SMIB system, complete with PSS and TCSC, can be obtained by linearizing the equations (12) through (16). (15). Figure 3 [19] illustrates the block diagram paradigm that corresponds to this figure.

2.4. Optimization method

The Shuffled Frog Leaping Algorithm (SFLA) is an evolutionary, meta-heuristic, memetic optimization algorithm that incorporates aspects of the Shuffled Complex Evolution Algorithm and the Particle Swarm Optimization [17]. SFLA is classified as an evolutionary, meta-heuristic, and memetic optimization algorithm. This algorithm has been implemented as a solution to a wide variety of optimization challenges, such as the knapsack problem, the traveling salesman problem, the optimization of water transportation networks [20], and the optimization of electrical power flow [18]. The SFLA algorithm has been successfully applied to a variety of difficult and multidimensional optimization problems. In the following portions, we will go over the fundamental SFLA procedure as well as its application in order to get the best possible TCSC controller parameters.

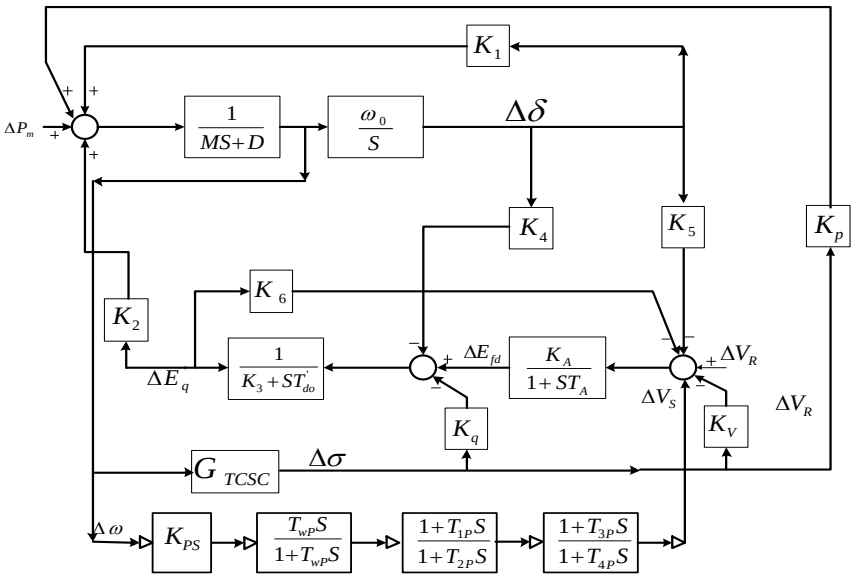

Figure 3. A Phillips-Heffron version of SMIB including TCSC as well as PSS

Initially, a set of X={x1,x2,….xn}f virtual frogs are randomly generated within the solution space, where each frog is represented by xi={xi1, xi2,…. xih}, where there are h variables. The set of variables are memo types of the meme, analogous to the chromosomes of genes. The frogs are evaluated with a fitness function and ranked in fitness order. The n frogs have been then sorted into m memeplexes, where x1 goes into the first memeplex,

xm goes into the mth memeplex, x_{m+1} goes into the first memeplex, etc. Once the memeplexes have been sorted, a local search process similar to the one used in particle swarm optimization is utilized. The best (xb) besides worst frog (xw) in each memeplex, as well as an overall best frog (xg) are identified.

$$D_i = rand \times (x_b - x_w), D_{min} \leq D_i \leq D_{max} \quad (19)$$

$$D_i = rand \times (x_g - x_w), D_{min} \leq D_i \leq D_{max} \quad (20)$$

$$x'_w = x_w + D_i \quad (21)$$

Where *rand* stands for a random variable [0,1], x'_w is new x_w, and D_i stands for step size for each *h* variable.

For each of the h variables of xw, a random step Di is determined for xw by Eq. 1. If this improves the worst frog fitness, then the improved frog, x_w' replaces x_w. If not, x_w is improved based on Eq. 2 which uses xg. If this is an improvement, then the new frog is kept. If neither Eq. 1 nor Eq. 2 provide improvement in fitness, then a random frog is created to replace xw. The complete population is reshuffled and then broken down into new memeplexes after a predetermined number of iterations, which is analogous to the method that is utilized in the shuffled complex evolution algorithm. The position of xg is brought up to speed, and the conditions necessary for convergence are examined. If xg does not change after a predetermined number of iterations of global shuffling, if a predetermined condition is satisfied, or if the maximum number of global iterations has been reached, these are typically considered to be convergence conditions. The steps involved in this process are outlined in Figure 1. There are a few different parameters for SFLA that need to be optimized for any given study. These include the number of frogs, the number of memeplexes, the number of iterations of local search conducted before shuffling, the maximum Di, and the number of global iterations or shuffles. Generally, the total population of frogs is found to be the most important parameter, proportional to the complexity of the problem, and max D_i is typically 100% [21]. The number of memeplexes, *m*, is around 10% of *n*, and the number of local iterations before shuffling is generally between *m/2* and *m x 2* and the number of global iterations is typically from 100 to 1000 [22]. It is advisable to test a variety of parameter settings for any SFLA algorithm to find the fastest convergence.

2.5. Improvements on basic SFLA

Although SFLA's combination of a global and local search results in fast convergence speeds, many authors have noted that the basic SFLA procedure is vulnerable to local extremum. As a result, several groups have developed modified SFLA for enhanced accuracy. Much research has been done on improvements to the SFLA. Broadly speaking, the incorporation of mutation factors, cooperation/sharing of meme types, incorporation of sub-memeplexes, the use of weighted inertia factors, and hybridizing SFLA with other algorithms such as PSO, ant colony optimization, genetic algorithm, and bacterial algorithms, are all viable routes. For example, to mitigate convergence to local extremum, Teekeng and Thammano created sub-memeplexes of frogs for local search, usually higher fitness frogs. In this way, a more diverse memeplex is created rather than simply improving the worst frog relative to the best frog. Another method to prevent local extremum convergence is through diversity, via mutation and cooperation. Wang, et. al. proposed a modified SFLA with an inertia weight to regulate the search area, a differential operator for diversification utilizing random points in a population, and sharing of memetypes between random frogs i.e. cooperation [23-26]. Indeed, the use of an inertia weight was inspired from the Particle Search Optimization (PSO), which utilizes a similar concept [26-30].

$$V_i' = \omega \times V_i + c_1 \times rand(X_p - X_i) + c_2 \times rand(X_g - X_i) \quad (22)$$

Where c1 and c2 are random constants, and rand are two random variables [0,1], V_i is current velocity, V_i' is new velocity, X_p is previous best position, X_q is the position of the best particle, and *w* stands for inertia weight. The *w* has a role for balancing global and local search. It has been proposed that the operator decreased linearly over time to allow for large global search in the beginning, and more local search later on, a concept that can be applied to SFLA. In our optimization problem the latter improvement by Wang, et. al. is applied to achieve superior results with less time. SFLA has been proven to be a versatile, high performing algorithm in comparison to other types of evolutionary algorithms, and has strong potential in all areas of optimization research.

2.6. Problem formulation

This research opts for the popular lead-lag configuration for both the PSS and TCSC controllers. Figure 2 and Figure 4 depict the ahead-of-the-pack and trailing-behind organizational patterns of the PSS and TCSC, respectively. Primary value of conduction angle and deviation from it are used to define the TCSC reactance. The TCSC time constant is denoted by TC. Gain and signal washout blocks, as well as a two-stage phase correction block, make up the TCSC under consideration here. The washout time constant T_{WT} is considered 10 sec in this study. The speed deviation Δω is inputted to the T_{CSC} stabilizer. Moreover, two parallel phase compensator blocks are considered so that T_{2T} = T_{4T} = 0.1 Sec. The rest of parameters (stabilizer gain K_{PT}, constants time T_{1T} and T_{3T}) to be obtained.

The TCSC's damping force can be broken down into direct and indirect components. The generator's electromechanical oscillation cycle is controlled by the direct-acting parameter K_P while K_Q and K_V which are the indirect parts are applied via field channel of the generator. The portion of the damping torque generated by the *TCSC* can be determined by:

$$\Delta T_D = T_D \omega_0 \Delta\omega \cong K_P K_T K_D \Delta\omega \tag{23}$$

Where, T_D is the damping torque coefficient. The transfer functions for PSS and the *TCSC* controllers are:

$$U_{PSS} = K_P \left(\frac{sT_{WP}}{1+sT_{WP}}\right)\left(\frac{1+sT_{1P}}{1+sT_{2P}}\right)\left(\frac{1+sT_{3P}}{1+sT_{4P}}\right)y \tag{24}$$

$$U_{TCSC} = K_T \left(\frac{sT_{WT}}{1+sT_{WT}}\right)\left(\frac{1+sT_{1T}}{1+sT_{2T}}\right)\left(\frac{1+sT_{3T}}{1+sT_{4T}}\right)y \tag{25}$$

Here, U_{TCSC} and U_{PSS} stand for the output signals for TCSC controller *y* stands for the signals that input to these controllers.

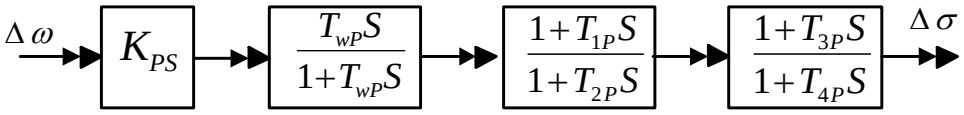

Figure 4. The lead-lag structure of the TCSC

2.7. Objective function

This study specifically concentrates on two contingencies in the network. Disturbance in mechanical power or disturbance in reference voltage is the most common reason of power oscillation in the network. However, it is worth mentioning that simultaneous occurrence of two or more disturbances in a network is extremely rare and consequently, they are studied separately. In order to minimize these oscillations and maximize stability against mentioned disturbances, PSS and TCSC controllers act in coordinated manner so that be able to damp these disturbances properly. One possible solution to trace the oscillations in the network is investigating the deviation in generator rotor speed (Δω). This could be happened by separate investigation on deviation in rotor speed for the identical inputs for either of aforementioned disturbances. In order to satisfy this goal, A common formulation for the objective function J is the reduction of:

$$\min J = \sum_i m_i \int_0^{t_1} t[\Delta\omega_i(t,x)]^2 d_t = m_1 \int_0^{t_1} t[\Delta\omega_1(t,x)]^2 d_t + m_2 \int_0^{t_1} t[\Delta\omega_2(t,x)]^2 d_t \tag{26}$$

Subject to: $x_{\min} < x < x_{\max}$

where, Δω(t,x) represents a rotor speed deviation for controller parameters X comprising K_{PT} , K_{PS} , T_{1T} , T_{3T} , T_{1P} , T_{3P} which should be tuned; t_1 is the time range of the simulation; and parameter m is the weighting factor of each case. The gain parameters (K_{PT} and K_{PS}) are specified in span of 0.01 to 500 while time constant parameters (T_{1T}, T_{3T} , T_{1P} , and T_{3P}) are selected in the interval of 0.01 and 3. Here, it is aimed to achieve a solution that can guarantee the system response against either disorder in mechanical power input or in reference

voltage based on settling time in addition to overshoot. In Eq.(26), the subscript 1 refers to disturbance in mechanical input; while subscript 2 is referring to the disturbance in reference voltage.

3. Results and discussion

Optimum tuning for PSS besides TCSC controller parameters in both independent and coordinated manner is a complex task, particularly due to the fact that many setting for controller can be done in an acceptable performance. Hence, application of an algorithm with property of escaping from local optimums is a key to attain the global optimum. This property, through defined operators, is embedded into the PSO-SFLA and discriminates it from its parents PSO and Shuffled Frog Leaping Algorithm [18]. In order to evaluate parameters suggested by the algorithm and calculate fitness value of parameters, two separate simulations are run. Firstly, a system dynamic version has exposed to a 5% step increasing in a mechanical power input (ΔPm) when t is 1.0 sec to calculate the first part of objective function (ΔPm = 5% ; ΔVR = 0). The second part of the objective function is calculated through another simulation by exerting a 5% step increase in the voltage reference (ΔVR) under t = 1.0 sec into a system (ΔPm = 0 ; ΔVR = 5%). The third case is a 3-phase self-clearing fault happens at a new 2 area 4 machine power system that has been explained in the next sections. Afterward, the objective function value is determined by adding these three quantities. The optimization process is stopped when the number of generations that was predetermined has been reached. For the purpose of optimization, one hundred generations were used, and the number of the population was held constant at forty. The behavior of the algorithm upon conclusion is depicted in Figure 5. The graph makes it abundantly obvious that coordinated design is superior to individual design in terms of reducing the goal function to its smallest possible value. Tables 1 and 2 demonstrate, respectively, the optimized controller parameters that were obtained through coordinated and individual design methods using the PSO-SFLA algorithm. These methods were used to design the controller.

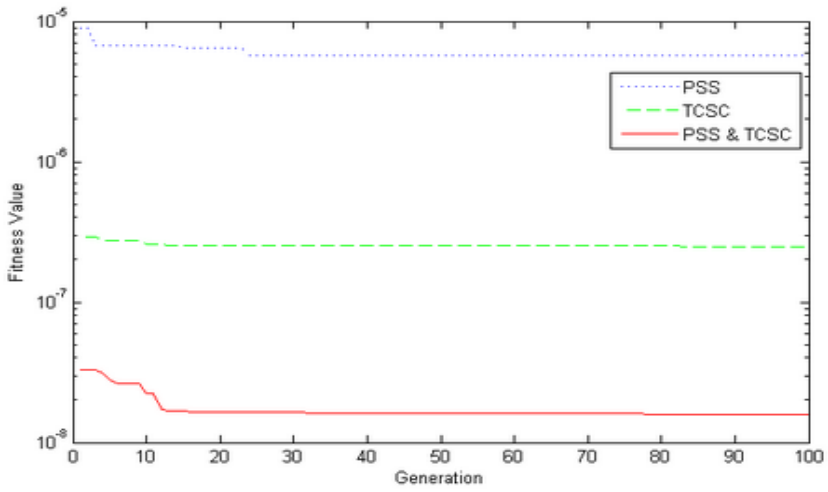

Figure 5. The convergence process for projected algorithm.

Table 1. The enhanced parameters for projected controllers for first case

PARAMETERES	Individual design		Coordinated design	
	PSS	TCSC	PSS	TCSC
K	45.0966	69.8469	58.3322	43.8743
T1	0.065	0.0101	0.0526	0.9329
T2	0.09	0.1	0.1	0.1
T3	0.4185	1.2204	0.2325	0.1139
T4	0.09	0.1	0.1	0.1

Table 2. The enhanced parameters for projected controllers for the second case

PARAMETERES	Individual design	Coordinated design	
	PSS	PSS	TCSC
K	1	1	47.821
T1	0.325	0.035	2
T2	0.008	0.0012	0.2
T3	0.045	0.089	0.0001
T4	0.065	0.0765	0.238

Table 3. System eigenvalues with and with no control

(Individual and synchronized design)

Without control	PSS only	TCSC only	Coordinated design
0.2453± 6.4340i	-0.0002± 25.4410i	-0.7127± 2.0774i	-1.5263± 1.9349i
-12.9256± 20.4470i	-1.5567± 2.4524i	-9.6406± 23.2916i	-8.3874± 23.8292i
-	-17.6093	-15.8653± 23.0035i	-11.4643
-	-0.1024	-0.1014	-52.3917
-	-24.6351	-	-10
-	-	-	-0.1042
-	-		-0.1

In the first instance, simulated SMIB system are run to compare a performance for PSS and TCSC controllers at taming erratic oscillations. Table 3 lists the eigenvalues of the system with and without the aforementioned regulators. Open loop systems are notoriously unreliable due to the lack of damping of the electromechanical mode. When PSS is used, the system is stabilized, and the eigenvalue of the electrical mode moves toward the left of the s=-0.0002 line in s-plane. The eigenvalue of the electromechanical mode is moved to the left of the line s = -0.7127 in the s-plane by a TCSC with a different design, which improves the system's stability and the mode's damping properties. This is an improvement over the PSS. However, the coordinated design method achieves the greatest stability, resulting in a significant movement of the electrical mode eigenvalue to the left of the line in the s-plane (s = -1.5263). The overall system's reliability is thus greatly improved. The aim of putting the system through its paces is to illustrate how the upgraded controllers have impacted it by showing how it reacts to different disturbances. Every perturbation is applied directly to a system at this point. In the first phase, a mechanical force input is increased by 5% at t = 1 second. Figure 6 illustrates the system's reaction to this scenario with PSS and TCSC controllers designed separately, together, and both independently. Although TCSC's standalone design works better than PSS's standalone design, coordinated design responses are superior to standalone designs when it comes to overshoot and settling time. With the coordinated design method, the settling time is drastically decreased, and the initial swing in the δ, ω and Pa has been considerably repressed. We also compare the PSS stabilizing signal (V_S) and TCSC controller transmission angle ($\Delta\sigma$) when they are designed separately and in concert (see Figures 7 and 8). The coordinated design scheme clearly outperforms the individual design of PSS, and it requires much less work to maintain stability. This proves the feasibility of a coordinated strategy for making full use of the control methods to improve a dynamic stability for a system.

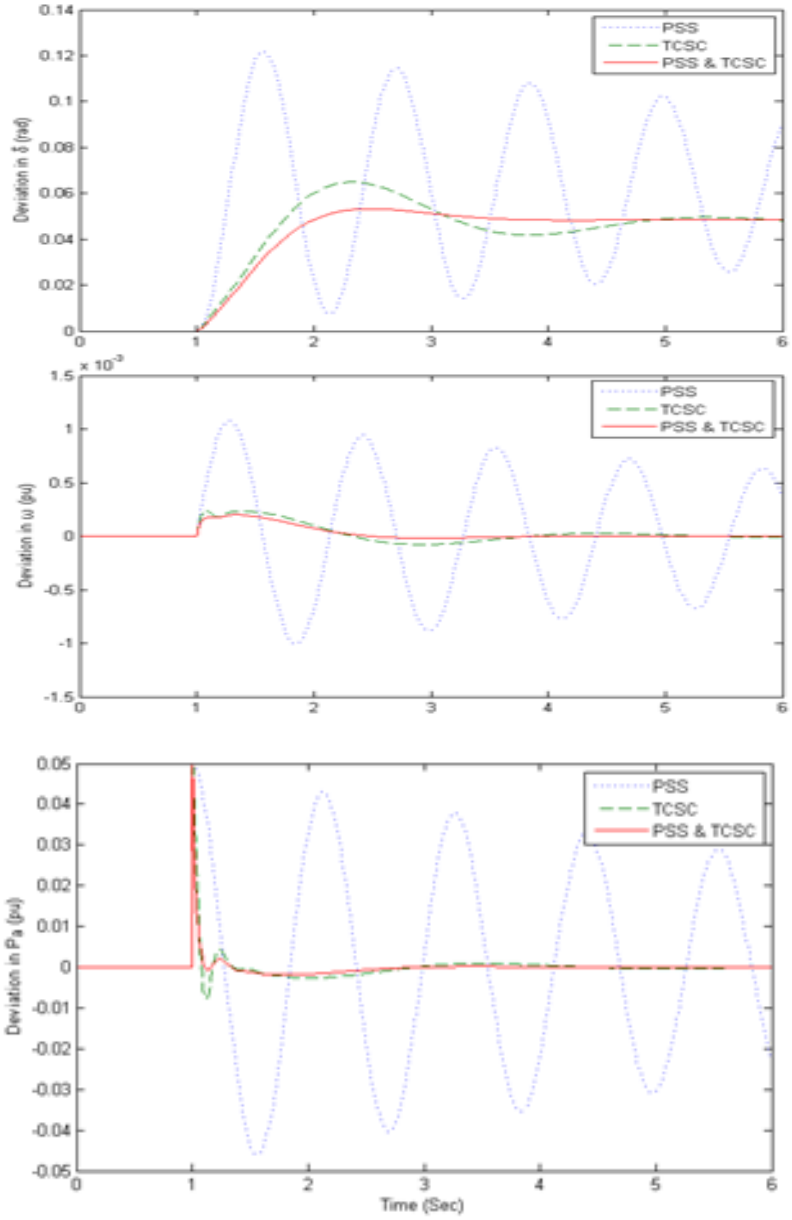

Figure 6. The system output in mechanical power input for 5% step increases

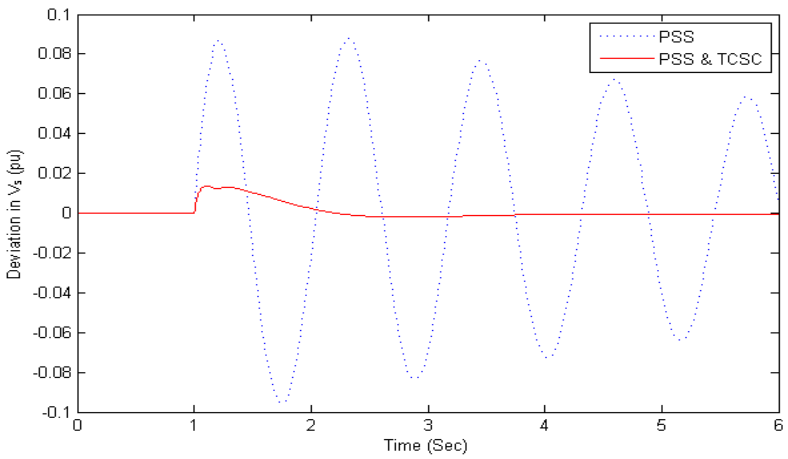

Figure 7. Stabilizing signal deviations for PSS (VS)

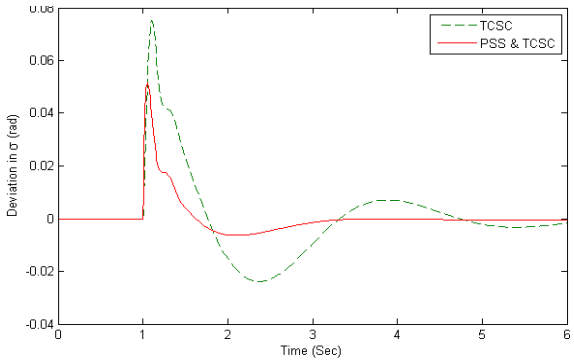

Figure 8. ($\Delta\sigma$) of the conduction angle of the controller TCSC

The second phase assesses a performance for suggested controllers in the presence of a reference voltage setting disturbance. At t = 1 sec, the reference voltage is raised by 5%. You can see how the system reacts in Fig. 9 when faced with the aforementioned scenario. The figure shows why a group effort is preferable to solo effort when it comes to designing. The coordinated design method's success can be traced back to the fact that it provides a quicker reaction than the individual method. The coordinated design method stabilizes the system much more quickly and has excellent damping features under low frequency oscillations. This increases a maximum safe transfer for energy and a margin stability of the electricity grid. Figures 10 and 11 show a comparison of the PSS stabilizing signal (VS) with the ((Δσ) the conduction angle of TCSC controller as considered separately and in a coordinated way, respectively. Coordinated design schemes clearly outperform the individual design of PSS, and they greatly reduce the required amount of control effort. This proves the feasibility of a coordinated strategy for making full use of the control methods to improve the dynamic stability of the system.

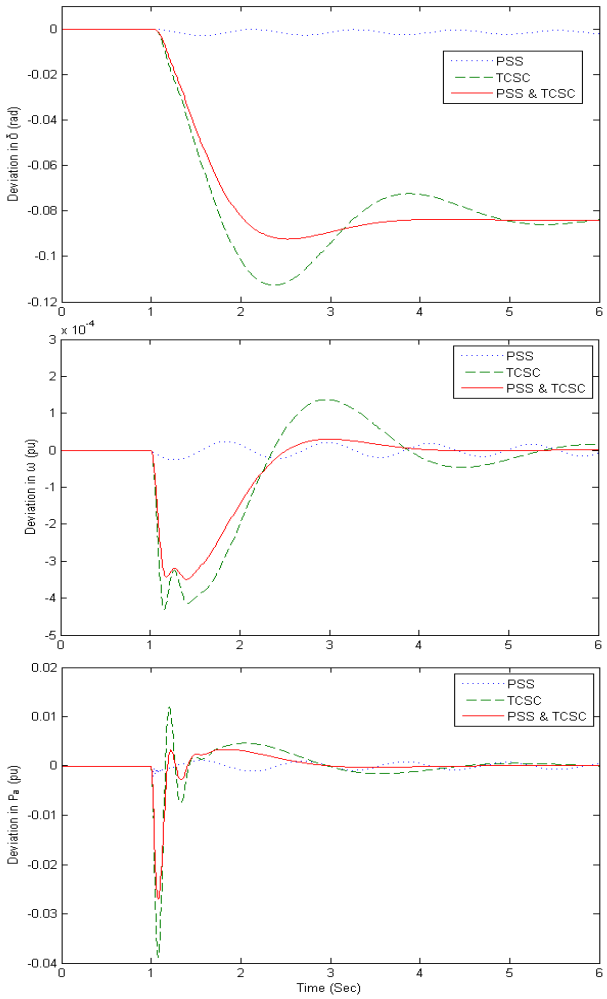

Figure 9. The system response for 5% step increases in reference voltage

In the 2nd case study, the projected technique is applied to a power system consisting of numerous machines and controllers. The research test bed is the two-area, four-machine benchmark system depicted in Fig. 12 with parameters as described in [1]. To regulate the current through the connection line between busses 8 and 9 and reduce vibrations, a TCSC has been installed there. However, extensive research is needed to determine the best spot for TCSC in real-world, large-scale power networks. The stability of the system in addition to an equilibrium between production and demand can be gauged in large part by measuring frequency.
These values, or their derivatives like rotor speeds and their rate of change, are typically used as the feedback signals for the damping device [31]. As in the preceding case study, $\Delta\omega = \omega_1 - \omega_3$ are selected as global feedback signals. If bus 8 experiences a three-phase self-clearing fault, it is believed that the fault will last for 200 milliseconds. The suggested damping controller is installed in the TCSC at a tie line connecting buses 8 and 9. The resulting animation is shown in Figure 13. Figures show that both methods can reduce post-fault oscillations, but coordinated design has a greater impact.

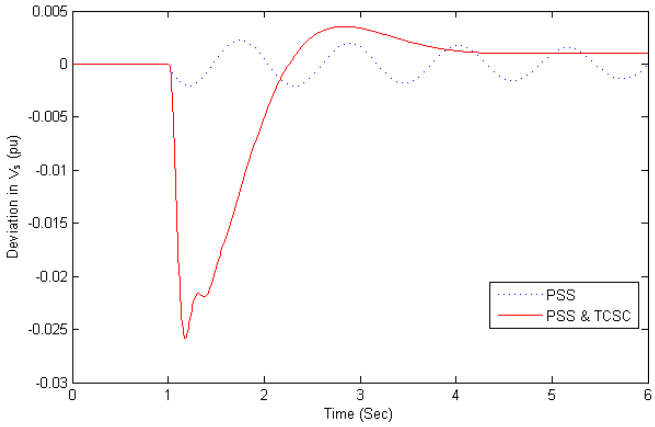

Figure 10. A stabilizing signal for PSS (V_S) for designed individually and in coordinated manner

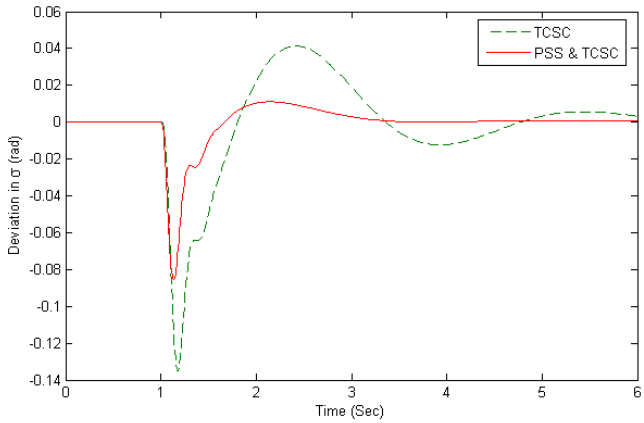

Figure 11. A conduction angle ($\Delta\sigma$) for TCSC controller for individually designed and in coordinated mode

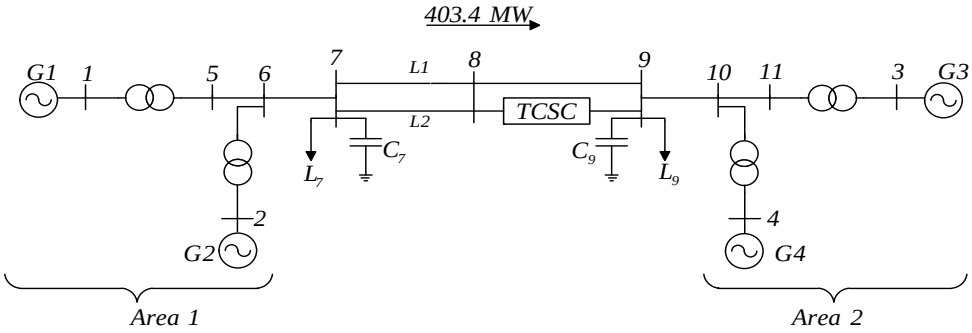

Figure 12. Two-area four-machine power system with TCSC

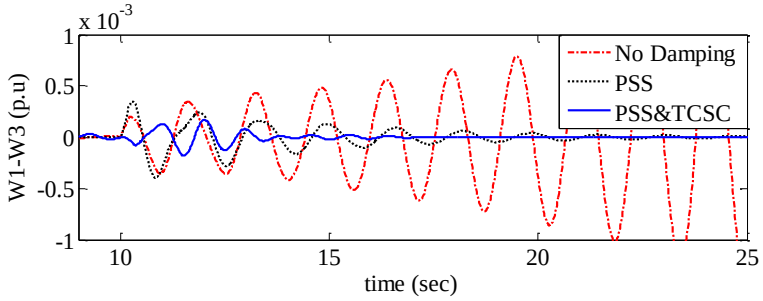

Figure 13. The system response at bus 8 for 200 ms for a 3-phase self-clearing fault

When compared to other methods currently in use, the simulation results above make it abundantly obvious that the suggested algorithm performed admirably. When compared to other current methods described in [23-25, 28-31], the convergence process time is found to be very fast and promising. In designing the PSS-TCSC Controller, it is clear that PSO-SFLA has outperformed in terms of accuracy, damping performance, minimum overshoot/undershoot response, and minimum settling time for both speed and rotor angle deviation responses. This further demonstrates the efficacy of our proposed approach. The results have been presented above. Microstrip filters and antennas can boost power wireless transmission as future trends [32-36].

4. Conclusion

In the course of this research, an innovative method for tuning the parameters of PSS and TCSC-based controllers was suggested with the goal of enhancing the level of stability of the SMIB power system. By using the rotor speed deviation as a criterion, the suggested optimization method was able to obtain optimal parameters of controllers both independently and in a coordinated fashion. Two potential disruptions were factored in independently into the goal function. Two disturbances were introduced into the system to test the results' effectiveness. For the former, we mulled over increasing the generator's mechanical input capacity by 5%. As for the second scenario, the standard voltage was raised by this amount. The results validated the coordinated design method as superior to the traditional methods of designing devices independently. In addition, coordinated design drastically cuts down on the volatile time. As a result, less work went into maintaining order. Through simulation, it was discovered that the PSO-SFLA algorithm is an efficient optimization instrument for dealing with problems of this kind. Although the focus of this study was on simulating a SMIB power system with PSS and TCSC, the algorithm that was developed can be used to simulate other types of FACTS devices in multi-machine systems. The authors intend to take this into consideration in their ongoing and future research.

Conflict of Interest

The authors declare that they have no conflict of interest and all of the authors agree to publish this paper under academic ethics.

Author Contributions

All the authors contributed equally to the manuscript.

Funding

The work was not supported by any official Institute or company, it completed by depended only on our efforts.

References

[1] P. S. Kundur and O. P. Malik, *Power system stability and control*. McGraw-Hill Education, 2022.
[2] P. Mattavelli, G. C. Verghese, and A. M. Stankovic, "Phasor dynamics of thyristor-controlled series capacitor systems," *IEEE Transactions on Power Systems*, vol. 12, no. 3, pp. 1259-1267, 1997.
[3] B. Li, Q. Wu, D. Turner, P. Wang, and X. Zhou, "Modelling of TCSC dynamics for control and analysis of power system stability," *International Journal of Electrical Power & Energy Systems*, vol. 22, no. 1, pp. 43-49, 2000.

[4] L. Fan, A. Feliachi, and K. Schoder, "Selection and design of a TCSC control signal in damping power system inter-area oscillations for multiple operating conditions," *Electric Power Systems Research,* vol. 62, no. 2, pp. 127-137, 2002.
[5] A. D. Del Rosso, C. A. Canizares, and V. M. Dona, "A study of TCSC controller design for power system stability improvement," *IEEE Transactions on Power Systems,* vol. 18, no. 4, pp. 1487-1496, 2003.
[6] F. T. Abed, and I. A. Ibrahim, "Efficient Energy of Smart Grid Education Models for Modern Electric Power System Engineering in Iraq," in *IOP Conference Series: Materials Science and Engineering*, 2020, vol. 870, no. 1: IOP Publishing, p. 012049.
[7] J. J. Sanchez-Gasca and J. H. Chow, "Power system reduction to simplify the design of damping controllers for interarea oscillations," *IEEE Transactions on Power systems,* vol. 11, no. 3, pp. 1342-1349, 1996.
[8] P. Pourbeik and M. J. Gibbard, "Simultaneous coordination of power system stabilizers and FACTS device stabilizers in a multimachine power system for enhancing dynamic performance," *IEEE Transactions on Power Systems,* vol. 13, no. 2, pp. 473-479, 1998.
[9] H. F. Khazaal, F. T. Abed, and S. I. Kadhm, "Water desalination and purification using desalination units powered by solar panels," *Periodicals of Engineering and Natural Sciences,* vol. 7, no. 3, pp. 1373-1382, 2019.
[10] A. A. Daleh Al-Magsoosi, and F. T. Abed, "Monitoring the Consumption of Electrical Energy Based on the Internet of Things Applications," *International Journal of Interactive Mobile Technologies,* vol. 15, no. 7, pp. 17-29, 2021.
[11] S. Panda and N. P. Padhy, "Coordinated design of TCSC controller and PSS employing particle swarm optimization technique," *International Journal of Electrical and Computer Engineering,* vol. 1, no. 4, pp. 706-714, 2007.
[12] S. B. Nejad, S. H. Elyas, A. Khamseh, I. N. Moghaddam, and M. Karrari, "Hybrid CLONAL selection algorithm with PSO for valve-point Economic load Dispatch," in *2012 16th IEEE Mediterranean Electrotechnical Conference*, 2012: IEEE, pp. 1147-1150.
[13] S. H. Elyas, P. Mandal, A. U. Haque, A. Giani, and T.-L. B. Tseng, "A new hybrid optimization algorithm for solving economic load dispatch problem with valve-point effect," in *2014 North American Power Symposium (NAPS)*, 2014: IEEE, pp. 1-6.
[14] M. Jafari, A. M. Shahri, and S. H. Elyas, "Optimal tuning of brain emotional learning based intelligent controller using clonal selection algorithm," in *ICCKE 2013*, 2013: IEEE, pp. 30-34.
[15] M. Valizadeh , I. ALRubeei, and F. Abed, "Enhancing the efficiency of photovoltaic power system by submerging it in the rivers," *Telkomnika (Telecommunication Computing Electronics and Control)*, vol. 20, no. 1, pp. 166-172, 2022.
[16] I. A. Aljazaery, and S. K. Al_Dulaimi, "Generation of High Dynamic Range for Enhancing the Panorama Environment," *Bulletin of Electrical Engineering* and Informatics, vol. 10, no. 1, 2021.
[17] H. Abdelwahed, "Demand Side Management- Literature Review and Performance Comparison," in *2019 11th International Conference on Computational Intelligence and Communication Networks (CICN)*, Honolulu, HI, USA, 2019.
[18] K. Padiyar, *Power system dynamics: stability and control*. John Wiley New York, 1996.
[19] H. Wang, F. Swift, and M. Li, "A unified model for the analysis of FACTS devices in damping power system oscillations. II. Multi-machine power systems," *IEEE Transactions on Power Delivery,* vol. 13, no. 4, pp. 1355-1362, 1998.
[20] M. Eusuff, K. Lansey, and F. Pasha, "Shuffled frog-leaping algorithm: a memetic meta-heuristic for discrete optimization," *Engineering optimization,* vol. 38, no. 2, pp. 129-154, 2006.
[21] A. Sarkheyli, A. M. Zain, and S. Sharif, "The role of basic, modified and hybrid shuffled frog leaping algorithm on optimization problems: a review," *Soft Computing,* vol. 19, no. 7, pp. 2011-2038, 2014, doi: 10.1007/s00500-014-1388-4.
[22] H.-b. Wang, K.-p. Zhang, and X.-y. Tu, "A mnemonic shuffled frog leaping algorithm with cooperation and mutation," *Applied intelligence,* vol. 43, pp. 32-48, 2015.
[23] X. Li, J. Luo, M.-R. Chen, and N. Wang, "An improved shuffled frog-leaping algorithm with extremal optimisation for continuous optimisation," *Information Sciences,* vol. 192, pp. 143-151, 2012.

[24] M. Mokhtari, F. Aminifar, D. Nazarpour, and S. Golshannavaz, "Wide-area power oscillation damping with a fuzzy controller compensating the continuous communication delays," *IEEE Transactions on Power Systems*, vol. 28, no. 2, pp. 1997-2005, 2012.
[25] S. Mahapatra and A. Jha, "PSS & TCSC coordinated design using particle swarm optimization for power system stability analysis," in *2012 2nd International Conference on Power, Control and Embedded Systems*, 2012: IEEE, pp. 1-5.
[26] R. Narne, P. Panda, and J. P. Therattil, "Genetic algorithm based simultaneous coordination of PSS and FACTS controllers for power oscillations damping," in *2012 IEEE Third International Conference on Sustainable Energy Technologies (ICSET)*, 2012: IEEE, pp. 85-90.
[27] F. T. Abed, N. K. Abed, and H. Salim, "Detection of power transmission lines faults based on voltages and currents values using K-nearest neighbors," *International Journal of Power Electronics and Drive Systems (IJPEDS)*, vol. 14, no. 02, pp. 1033-1043, 2023.
[28] D. S. Hasan, "Impact of Temperature and Dust Deposition on PV Panel Performance," in *AIP conference proceedings*, 2021, vol. 2394, no. SICPS2021: AIP Publishing LLC.
[29] H. T. Salim, and M. Suker, "Using Internet of Things application for Monitoring Photo-Voltaic Panel Based on Ask Sensors Cloud," *Design Engineering*, pp. 3884-3896, 2021.
[30] M. H. Majhool, and M. S. Farhan, "Design and implementation of sunlight tracking based on the Internet of Things," in *IOP Conference Series: Earth and Environmental Science*, 2021, vol. 877, no. 1: IOP Publishing, p. 012026.
[31] B. S. Theja, A. Raviteja, A. Rajasekhar, and A. Abraham, "Coordinated design of power system stabilizer using thyristor controlled series compensator controller: An artificial bee colony approach," in *2012 International Conference on Communication Systems and Network Technologies*, 2012: IEEE, pp. 606-611.
[32] Y. S. Mezaal, H. T. Eyyuboglu, and J. K. Ali, "A novel design of two loosely coupled bandpass filters based on Hilbert-zz resonator with higher harmonic suppression," in *2013 Third International Conference on Advanced Computing and Communication Technologies (ACCT)*, 2013.
[33] S. A. Shandal, Y. S. Mezaal, M. F. Mosleh, and M. A. Kadim, "Miniaturized wideband microstrip antenna for recent wireless applications," *Adv. Electromagn.*, vol. 7, no. 5, pp. 7–13, 2018.
[34] Y. S. Mezaal and H. T. Eyyuboglu, "A new narrow band dual-mode microstrip slotted patch bandpass filter design based on fractal geometry," in *7th International Conference on Computing and Convergence Technology (ICCIT, ICEI and ICACT)*, 2012, pp. 1180–1184.
[35] Y. S. Mezaal, H. H. Saleh, and H. Al-saedi, "New compact microstrip filters based on quasi fractal resonator," *Adv. Electromagn.*, vol. 7, no. 4, pp. 93–102, 2018.
[36] F. Abayaje, S. A. Hashem, H. S. Obaid, Y. S. Mezaal, and S. K. Khaleel, "A miniaturization of the UWB monopole antenna for wireless baseband transmission," *Periodicals of Engineering and Natural Sciences*, vol. 8, no. 1, pp. 256–262, 2020.

Appendix 1: Derivation of the constants

Values of the variables with subscript 0 are their pre-disturbance steady-state amount.

$$i_{q0} = \frac{P_0 V_{to}}{\sqrt{(P_0 x_q)^2 + (V_{to}^2 + Q_0 x_q)^2}} \quad (19)$$

$$v_{d0} = i_{q0} x_q \quad (20)$$

$$v_{qo} = \sqrt{V_{t0}^2 - v_{t0}^2} \quad (21)$$

$$i_{d0} = \frac{Q_0 + x_q i_{q0}^2}{v_{q0}} \quad (22)$$

$$E_{q0} = v_{q0} + i_{d0} x_q \quad (23)$$

$$E_0 = \sqrt{(v_{d0} + x_e i_{q0})^2 + (v_{q0} - x_e i_{d0})^2} \quad (24)$$

$$\delta_0 = \tan^{-1} \frac{(v_{d0} + x_e i_{q0})}{(v_{q0} - x_e i_{d0})} \quad (25)$$

$$K_1 = \frac{x_q - x_d'}{x_e + x_d'} i_{q0} E_0 \sin(\delta_0) + \frac{E_{q0} E_0 \cos(\delta_0)}{x_e + x_q} \quad (26)$$

$$K_2 = \frac{E_0 \sin(\delta_0)}{x_e + x_d^{'}} \tag{27}$$

$$K_3 = \frac{x_d^{'} + x_e}{x_d + x_e} \tag{28}$$

$$K_4 = \frac{x_q - x_d^{'}}{x_e + x_d^{'}} E_0 \sin(\delta_0) \tag{29}$$

$$K_5 = \frac{x_q}{x_e + x_q} \frac{v_{d0}}{V_{t0}} E_0 \cos(\delta_0) - \frac{xd^{'}}{x_e + x_d^{'}} \frac{v_{q0}}{V_{t0}} E_0 \sin(\delta_0) \tag{30}$$

$$K_6 = \frac{x_e}{x_e + x_d^{'}} \frac{v_{q0}}{V_{t0}} \tag{31}$$

Nomenclature

X_{L1}, X_{L2}	Transmission lines reactance	V_T	Terminal voltage for generator
X_t	Reactance of the transformer	v_i	Velocity of the i^{th} particle
V_t	Generator terminal voltage	x_i	Position of the i^{th} particle
V_b	infinite bus voltage	N_c	Number of clones
δ	Rotor angle for generator	β	The multiplying factor
ω	Rotor speed for generator	N	Total number of antibodies
D	Damping constant for generator	c'	Mutated antibody of c
P_m	Mechanical input power for generator	$N(0,1)$	zero mean of gaussian random variable and standard deviation $\sigma=1$
P_e	Electrical output power for generator		
$E_q^{'}$	Transient EMF in q-axis for generator	ρ	Decay controller of the exponential function
E_{fd}	Field voltage		
$T_{do}^{'}$	Open circuit field time constant	f	Fitness of an individual normalized in the interval [0, 1]
T_A	Time constant of the excitation system		
K_A	The excitation system gain	c_1, c_2	Positive learning factor constants
X_e	Equal reactance of the system	φ_1, φ_2	Distributed random numbers on the interval [0, 1]
x_d	d-axis reactance of the generator		
$x_d^{'}$	d-axis transient reactance for generator	$p_i(t)$	The i^{th} particle's best position
x_q	q-axis reactance for generator	$p_g(t)$	The overall best position of the population
V_R	Reference voltage	T_D	Damping torque coefficient
V_{Td}	d-axis terminal voltage for generator	U_{PSS}	Output signal of the PSS
V_{Tq}	q-axis terminal voltage for generator	U_{TCSC}	Output signal of the TCSC-based stabilizer
K_C	Gain of the TCSC	T_C	Time constant of the TCSC